Electroactive controlled release thin films

Kris C. Wood*, Nicole S. Zacharia†, Daniel J. Schmidt*, Stefani N. Wrightman*, Brian J. Andaya‡, and Paula T. Hammond*§

Departments of *Chemical Engineering and †Materials Science and Engineering, Massachusetts Institute of Technology, Cambridge, MA 02139; and ‡Department of Chemical Engineering, University of Rochester, Rochester, NY 14627

Edited by David A. Tirrell, California Institute of Technology, Pasadena, CA, and approved December 10, 2007 (received for review July 25, 2007)

We present the fabrication of nanoscale electroactive thin films that can be engineered to undergo remotely controlled dissolution in the presence of a small applied voltage (+1.25 V) to release precise quantities of chemical agents. These films, which are assembled by using a nontoxic, FDA-approved, electroactive material known as Prussian Blue, are stable enough to release a fraction of their contents after the application of a voltage and then to restabilize upon its removal. As a result, it is possible to externally trigger agent release, exert control over the relative quantity of agents released from a film, and release multiple doses from one or more films in a single solution. These electroactive systems may be rapidly and conformally coated onto a wide range of substrates without regard to size, shape, or chemical composition, and as such they may find use in a host of new applications in drug delivery as well as the related fields of tissue engineering, medical diagnostics, and chemical detection.

drug delivery | layer-by-layer thin film | polymer | responsive materials | Prussian Blue

Recently, great interest has centered on the development of "smart" controlled release systems capable of administering drugs in response to external stimuli (e.g., electric or magnetic fields) for use in applications such as controlled release implants ("pharmacy-on-a-chip") (1–3). Toward these goals, microfabricated devices have been developed that make use of micrometer-scale pumps, channels, and wells to deliver drugs on demand (1–5). However, although these technologies have resulted in encouraging new treatment possibilities, several challenges still remain. For example, the direct integration of these systems into nonplanar, functional, or structural implants such as arterial stents, medical sutures, and bone prostheses is challenging because photolithographic and micromachining techniques are primarily developed for planar substrates (6). Furthermore, the multistep processing of these systems can be both time-consuming and expensive (7). In this article, we demonstrate the fabrication of ultrathin films made from nontoxic, FDA-approved materials that can undergo remotely controlled dissolution to release precise quantities of drugs or other agents in response to a small applied voltage (+1.25 V). These nanoscale systems can be used to conformally coat surfaces of virtually any shape, size, or chemical composition.

Electroactive thin films are constructed by using the layer-by-layer (LbL) directed self-assembly technique, which utilizes the alternating adsorption of materials containing complementary charged or functional groups onto a solid substrate to form thin films (8). This method can be used to create highly tunable, conformal thin films with nanometer-scale control over film composition and structure. The only criterion for inclusion in an LbL thin film is that the species of interest either possesses or can be encapsulated in a "carrier" species (i.e., nanoparticle, micelle, dendrimer, etc.) that possesses the desired complementary functional group. Thus, a wide range of components including polymers, proteins, nucleic acids, small molecules, and nanoparticles have been incorporated into these assemblies, which can further be constructed in a range of geometries and patterns (9, 10). As a result of this versatility, LbL thin films have been used in a variety of biological applications such as biomimetics, biosensors, functionalized membranes, coatings with antibacterial, antiinflammatory, and antifouling properties, arrays, and materials for directed protein and cell adhesion (reviewed in ref. 11). They have also been used extensively in drug delivery, most notably as films or microcapsules that can release drugs passively (12–15) or in response to environmental stimuli such as pH, ionic strength, or enzymes (11, 16–25).

The electroactive component of our films is Prussian Blue (PB), a nontoxic, FDA-approved inorganic iron hexacyanoferrate compound that is well known for its electrochromic (26), electrochemical (27), and magnetic properties (28). PB exhibits a number of stable oxidation states known colloquially as Prussian White (PW), Prussian Blue (PB), Berlin Green (BG), and Prussian Brown (PX), in order of increasing oxidation state. These states are all negatively charged with the exception of PX, which is neutral (29). PB can be synthesized in the form of polydisperse, anionic nanoparticles (median size 4–5 nm) that are stable in aqueous solution and can be incorporated into LbL films (30). Applying a potential of +1.25 V [compared with the saturated calomel electrode (SCE)] switches these materials between the PB (negative) and PX (neutral) states (30).

Here, we demonstrate that by applying a low voltage to PB nanoparticle-based LbL thin films, and thus changing the PB oxidation state from negative to zero-valent, we can induce rapid film destabilization and controlled release of the film's components. Destabilization leads to the release of the film's components into solution, and we quantify this controlled release using a model, radiolabeled compound [^{14}C-dextran sulfate (^{14}C-DS)]. We further show that this release is well controlled; that is, removal of the oxidizing potential results in restabilization of the remaining film, allowing for the release of precise quantities of material from a single film as well as "on–off" switching between stable and unstable states. Finally, as a measure of biocompatibility, we demonstrate that PB particles exhibit no measurable toxicity on a panel of mammalian cell lines at concentrations up to 1.0 mg/ml. Together, this technology represents a robust, inexpensive, and versatile platform for the fabrication of field-activated (remote-controlled) controlled release systems.

Results and Discussion

Electroactive LbL thin films are constructed as follows. A glass substrate coated with a conducting film of indium tin oxide

Author contributions: K.C.W., N.S.Z., and D.J.S. contributed equally to this work; K.C.W., N.S.Z., D.J.S., and P.T.H. designed research; K.C.W., N.S.Z., D.J.S., S.N.W., and B.J.A. performed research; K.C.W., N.S.Z., D.J.S., and P.T.H. analyzed data; and K.C.W. and P.T.H. wrote the paper.

The authors declare no conflict of interest.

This article is a PNAS Direct Submission.

§To whom correspondence should be addressed. E-mail: hammond@mit.edu.

This article contains supporting information online at www.pnas.org/cgi/content/full/0706994105/DC1.

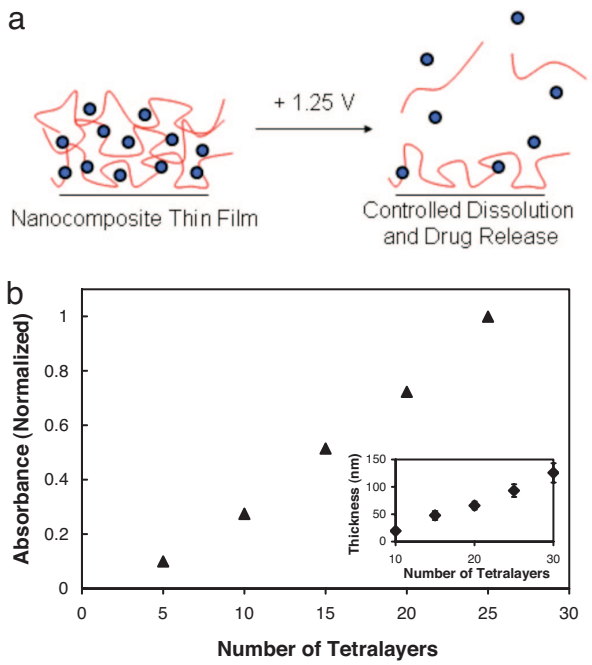

Fig. 1. Fabrication of LbL nanocomposite thin films based on PB. (*a*) Generalized schematic detailing the deconstruction of PB-based films containing drugs or other chemical species [blue circles represent PB nanoparticles and red lines represent drugs or chemical species (with or without a second encapsulating species)]. (*b*) Absorbance (700 nm) versus number of deposited tetralayers for the (LPEI/PB/LPEI/^{14}C-DS)$_{30}$ system as determined by UV-vis spectroscopy. Absorbance values are normalized to the absorbance of a 25-tetralayer film. (*Inset*) Thickness (nm) versus number of deposited tetralayers in the same system as determined by profilometry. Measurements were performed at six predetermined spots on the surface of the films, and error bars represent one standard deviation in measured values.

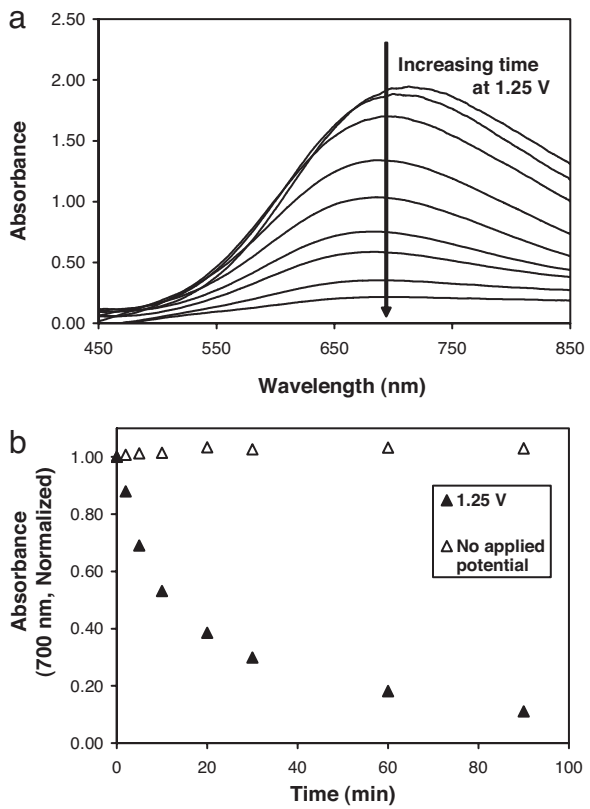

Fig. 2. Electrochemically induced deconstruction of (LPEI/PB/LPEI/^{14}C-DS)$_{30}$ films. (*a*) Absorbance spectrum showing decreasing PB absorbance with increasing time at 1.25 V. (*b*) Normalized absorbance (700 nm) versus time for films with (filled triangles) and without (open triangles) an applied potential.

(ITO) is first dipped in a solution containing a cationic drug or drug-containing "carrier" species and then rinsed in deionized water. Next, the substrate is dipped into an aqueous PB solution at pH 4 and rinsed again in deionized water. The process is repeated to build up a multilayer nanocomposite film with desired properties (see *Materials and Methods*). Controlled film deconstruction occurs upon the application of an electrochemical potential of 1.25 V, "switching" PB to the neutral PX state and destabilizing the film to release its encapsulated components (Fig. 1*a*). For details on the synthesis and structure of PB nanoparticles, see *Materials and Methods*, supporting information (SI) Fig. 6, and *SI Text*.

Fig. 1*b* shows the linear build-up of the tetralayer system containing linear poly(ethylenimine) (LPEI)/PB/LPEI/^{14}C-DS used in this study (measured by profilometry and UV-visual spectroscopy). Tetralayer systems, rather than traditional bilayer systems, were used to encapsulate and release ^{14}C-DS, our negatively charged model compound. The thickness of an average tetralayer was 4.2 ± 0.6 nm. (This value reflects the average of six data points taken at various positions on the surface of the film.) Films were observed to grow linearly in thickness with increasing numbers of layers. The linear growth behavior observed in these systems may have important implications for the controlled delivery of precise quantities of drugs or other agents because the thickness (and mass) of a given layer can be precisely predicted with no dependence on the thickness of the underlying film, resulting in facile control over release payloads.

Fig. 2 shows the deconstruction of (LPEI/PB/LPEI/^{14}C-DS)$_{30}$ films under the influence of an applied voltage held constant at 1.25 V, as monitored by UV-visual spectroscopy (PB exhibits an absorbance maximum at ≈700 nm). Absorbance from PB-containing films was observed to decrease with increasing amounts of time at 1.25 V (Fig. 2*a*). Quantitatively, absorbance at 700 nm was observed to decline rapidly during the first 5–10 min, reaching a value equal to 54% of that of the original film by 10 min (see Fig. 2*b*). Thereafter, absorbance continued to decrease, reaching a value of 38.5% of the original film by 20 min, 18.2% by 60 min, and 10.4% by 90 min. Absorbance measurements taken from a control film (no applied potential) showed no decrease in color, suggesting that PB loss is directly related to film instabilities that are stimulated by the applied potential. Total film thickness measurements demonstrate a decrease in film thickness with time (at 1.25 V) that is analogous to PB loss, suggesting that the loss of PB from films is associated with destabilization and deconstruction of the film structure (SI Fig. 7 and *SI Text*). The observed film destabilization is likely to be based on the loss of electroneutrality occurring within the film after the PB-to-PX transition, which results in the repulsion of adjacent, like-charged layers; similar mechanisms of film destabilization based on interlayer charge repulsion have been cited in the past (30, 31).

To determine whether the electrochemical destabilization of PB-containing films causes release of the film's components into solution, we built films containing a radiolabeled, model compound, ^{14}C-DS. Fig. 3*a* shows that these systems release ^{14}C-DS rapidly after the application of 1.25 V (for 30 min), with kinetics occurring over the same time scale as PB loss and total film degradation. To verify that release occurs only in the presence of an applied potential, we soaked films in a solution

CHEMISTRY

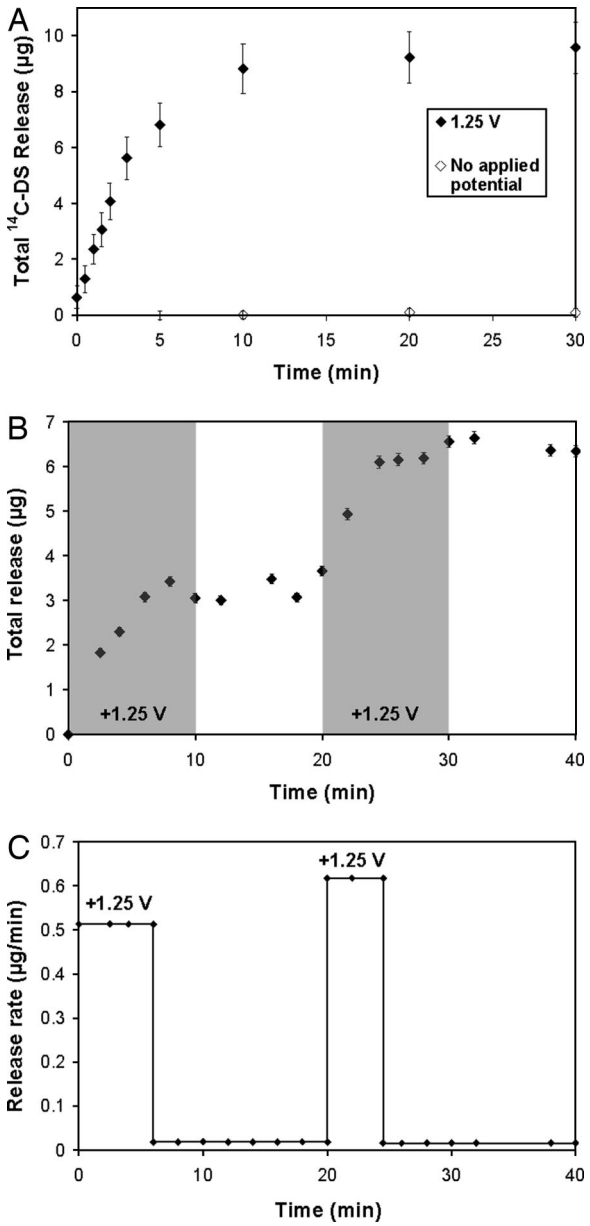

Fig. 3. Release of a model compound, ^{14}C-DS, from PB-containing films held at a constant potential of 1.25 V. All films are (LPEI/PB/LPEI/^{14}C-DS)$_{30}$. (*a*) Films held constant at 1.25 V (filled diamonds) or no applied potential (open diamonds) are shown. (*b*) Serial ^{14}C-DS release from two (LPEI/PB/LPEI/^{14}C-DS)$_{30}$ films in a single solution. One film was held at the oxidizing potential for 10 min, followed by 10 min below the oxidizing potential. Next, the process was repeated with a second film in the same degradation bath. Periods during which an oxidizing potential was applied are shaded.¶‖ (*c*) Release rate versus time for the films in *b*.** In all cases, error bars represent one standard deviation in measured values.

identical to those used in the deconstruction experiments (10 mM KCl) and observed no significant passive ^{14}C-DS release. Moreover, (LPEI/^{14}C-DS)$_{30}$ films lacking PB are stable in the presence of an applied potential of 1.25 V, exhibiting negligible ^{14}C-DS release and verifying our hypothesis that film destabilization is mediated by a valency state change in PB. Preliminary experiments also suggest that films exhibit similar stability and voltage-controlled release properties to those above in 10% serum-containing solutions (data not shown). (For a description of ^{14}C-DS release from films held at potentials below 1.25 V and analysis of current and power requirements in electroactive thin films, we refer the reader to SI Figs. 8–11 and *SI Text*.)

The ability of PB-containing thin films to release their contents only in response to a small applied potential suggests that these systems might be interesting materials for implantable pharmacy-on-a-chip applications (1). For example, existing patterning and machining techniques could be used to array multiple films onto individually addressable electrodes on a single substrate, and the application of a potential to individual films could result in the release of an active species from one film at a time. As a simple proof of this concept, we placed two (LPEI/PB/LPEI/^{14}C-DS)$_{30}$ films in a release bath and then applied a potential of 1.25 V to each film individually for 10 min (the time required to release each film's entire contents). As shown in Fig. 3 *b* and *c*, this results in the release of the contents of the first film followed by the contents of the second film. These results also suggest that the application of voltage to, and subsequent degradation of, the first film does not affect the release properties of the second film.

To more closely examine the kinetics of film deconstruction, we measured ^{14}C-DS release from representative 30-tetralayer LPEI/PB/LPEI/^{14}C-DS systems under the influence of a square wave potential of 1.25 V for varying amounts of time. In Fig. 4*a*, the total ^{14}C-DS release from films held at the oxidizing potential for differing time intervals is shown. Films release significantly more ^{14}C-DS after 10- and 30-min intervals than shorter 10-s or 1-min intervals, an indication of the on–off switchable nature of film destabilization. Furthermore, 10- and 30-min intervals result in similar quantities of release with similar kinetics (data not shown), suggesting that all of the available ^{14}C-DS was released within the first 10 min (all films were deposited onto identical ITO-coated glass substrates from the same dipping solutions to ensure uniform thickness and ^{14}C-DS loading). To examine whether films can be switched between stable and unstable states, a single film was exposed to two 1-min intervals at 1.25 V, separated by a 14-min interval without an applied oxidizing potential (see Fig. 4 *b* and *c*). Release profiles indicate that films are rapidly destabilized in the presence of an oxidizing potential, then restabilized when the potential is removed. This process can be reversed, because reapplication of the oxidizing potential can again destabilize the film. From these data, it is apparent that the stability (and controlled release properties) of PB-based films can be precisely controlled electrochemically. In drug delivery applications, this on–off switchable stability may allow for an additional means of fine-tuned control over doses administered from implanted films. Together, the data in Fig. 4 suggest the following: (*i*) the process of film destabilization can be switched off by removing the oxidizing potential and reactivated by reapplying the potential; (*ii*) diffusion of the film's components out of the destabilized film structure, rather than valency state switching in PB, is the rate-limiting step in film degradation (because PB redox switching times in these systems are ≈15–20 s) (SI Fig. 9 and *SI Text*); and (*iii*) deconstruction and release from 30-tetralayer systems is completed in <10 min when held at constant oxidizing potential.

¶After holding at the oxidizing potential of 1.25 V for the indicated time intervals, a potential of 0.6 V was applied to accelerate the reversion of PX back to its fully charged PB state.

‖Differences in total mass release between films used in *a* and *b* are due to slight variations in the pH and ionic strength of dipping baths used during the deposition processes.

**Release rates are calculated by using a simple linear fit of the increasing and plateau regions of the release curve.

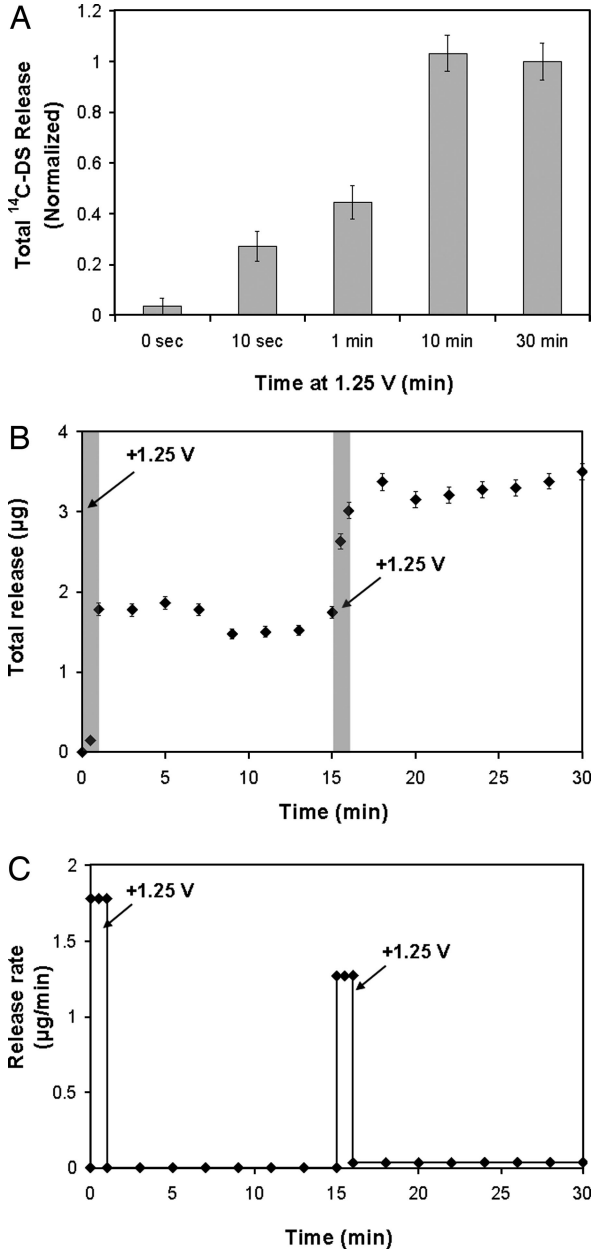

Fig. 4. On–off switchable destabilization of PB-containing (LPEI/PB/LPEI/^{14}C-DS)$_{30}$ films. (*a*) Total ^{14}C-DS release from equivalent samples held at the oxidizing potential of 1.25 V for varying times (normalized to total release at 30 min). (*b*) ^{14}C-DS release from a single film held at 1.25 V for 1-min intervals at $t = 0$ and 15 min.¶ (*c*) Release rate from film shown in *b*.** In all cases, error bars indicate one standard deviation in measured values.

Finally, as a measure of the biocompatibility of PB nanoparticles, we measured their toxicity on a panel of mammalian cell lines, including hepatocellular carcinoma (HCC), ovarian cancer (HeLa), and kidney fibroblast (Cos-7) cells, using a conventional 3-(4,5-dimethylthiazolyl-2)-2,5-diphenyltetrazolium bromide (MTT) assay. The MTT assay measures the effect of added substances on cell growth and metabolism, and is commonly used as an *in vitro* measure of toxicity (32). Interestingly, PB particles caused no observable toxicity at all concentrations tested (up to 1.0 mg/ml) in this assay, which can sensitively detect toxic effects of added substances (Fig. 5) (33). These findings are not surprising because PB is known to

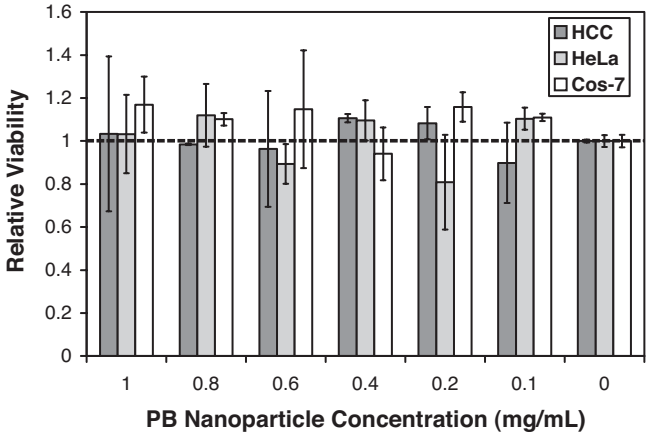

Fig. 5. MTT assay for cellular toxicity indicates that PB nanoparticles exhibit no toxicity on three different cell lines at concentrations up to 1.0 mg/ml. Error bars represent one standard deviation in measured values.

cause no adverse health effects in humans and was approved by the United States FDA in 2003 for the treatment of radiation contamination and heavy metal poisoning (34). For more information on toxicity studies involving PB-based electroactive thin films, please see *SI Text*.

Conclusions

We have demonstrated an approach for constructing nanostructured thin films capable of releasing precise quantities of compounds on demand in response to small electrochemical potentials. Furthermore, we have shown that the films are stable enough to release a fraction of their contents and then restabilize upon removal of the applied potential. The LbL technique is sufficiently general to allow for the incorporation of drugs and agents of any structure (small molecules, macromolecules, charged and uncharged species, etc.) into these systems, alone or in conjunction with a "carrier" species (8–10). As a simple proof of principle, we have studied the (LPEI/PB/LPEI/^{14}C-DS) system, in which the biomolecule of interest (dextran sulfate) is alternately deposited [in conjunction with a "carrier" species (LPEI)] with the electroactive component, PB. Finally, we have outlined a mechanistic hypothesis to explain the deconstruction process occurring in these systems, whereby an electrochemical signal oxidizes the nanoparticles to the PX state, resulting in loss of particle charge and destabilization of the film through self-repulsion of the polycation species. We expect that these electroactive controlled release thin films may find interesting applications in fields including drug delivery, tissue engineering, medical diagnostics, analytical chemistry, and chemical detection. Furthermore, using the various thin film patterning techniques developed in recent years, we suggest that these materials may eventually be arrayed to produce multidrug or multidose "smart" devices (1).

Materials and Methods

^{14}C-dextran sulfate sodium salt (^{14}C-DS) (100 μCi, 1.5 μCi/mg, M_n = 8,000) was obtained from American Radiolabeled Chemicals. Linear poly(ethylenimine) (LPEI) (M_n = 25,000 or M_n = 250,000) was received from Polysciences. $FeCl_2$, potassium ferricyanide, and KCl were purchased from Aldrich. All materials and solvents were used as received without further purification.

Synthesis of PB nanoparticles proceeded as follows. Briefly, 35 ml of 10 mM aqueous $FeCl_2$ was added dropwise to an equivalent volume of 50 mM potassium ferricyanide and 50 mM KCl, agitated for 1 min, and filtered continuously with deionized water (with magnetic stirring) against a 3,000-Da cut-off regenerated cellulose membrane. Permeate solutions (containing 10 or more equivalent volumes) were yellow, suggesting that only the excess

potassium ferricyanide along with a trivial amount of PB may have passed through the membrane. The retentate solution was collected, pH-adjusted to 4 by addition of either potassium hydrogen phthalate buffer or HCl and NaOH, and used immediately in LbL assembly (30). The final concentration of PB in the dipping solution was ≈1.5 mg/ml.

LbL films were assembled on conducting ITO-coated glass substrates (Delta Technologies; 7 × 50 × 0.7-mm cuvette slide, 8- to 12-Ω resistance) for profilometry, spectroscopy, deconstruction, and release studies. ITO-glass substrates were cleaned via ultrasonication in dichloromethane, acetone, methanol, and deionized water for 15 min each, followed by a 5-min oxygen plasma etch (Harrick PCD 32G) to ensure that the surfaces were clean and abundant in hydroxyl groups. Dextran sulfate and LPEI dipping solutions were prepared at concentrations of 10 mM with respect to the polymer repeat unit in acetate buffer [100 mM (pH 5.1)] and deionized water (pH 4.0 by addition of HCl), respectively. Deionized water used to prepare all solutions was obtained by using a Milli-Q Plus at 18.2 MΩ.

LbL films were constructed as follows according to the alternate dipping method by using an automated Zeiss HMS Series programmable slide stainer (8). Briefly, pretreated substrates were submerged in an LPEI dipping solution for 10 min followed by a cascade rinse cycle consisting of three deionized water rinsing baths at pH 4.0 (15, 30, and 45 s, respectively). Substrates were then submerged in a PB dispersion for 10 min followed by the same cascade rinsing cycle, and the entire process was repeated as desired to construct (LPEI/PB) films with the desired numbers of layer pairs. Tetralayer films containing LPEI/PB/LPEI/^{14}C-DS were constructed by using the same general protocol; however, in this case, the PB dipping step alternated with a DS dipping step (10 min with cascade rinse cycle). Tetralayer systems were capped with a single layer of LPEI after the last deposition step. After deposition, films were immediately removed from the final rinsing bath and dried thoroughly under a stream of dry nitrogen gas. Film thickness and deconstruction experiments on conducting ITO-glass substrates were conducted by using a Tencor P10 profilometer by scoring the film and profiling the score. A tip force of 5 mg was used to avoid penetrating the polymer film.

Electrochemical deconstruction studies and chronoamperometry were performed by using an EG&G 263 A potentiostat/galvanostat with a three-electrode setup in a beaker. The electrolyte was a 10 mM KCl solution in deionized water (40-ml volume). The working electrode was an LbL film assembled on a conducting ITO-glass substrate (Delta Technologies; 7 × 50 × 0.7-mm cuvette slide, 8- to 12-Ω resistance), the reference electrode was a K-type saturated calomel electrode (SCE), and the counter electrode was a piece of Pt foil (2.5 × 2.5 cm). Chronoamperometry was performed by stepping between the open circuit potential (≈0.27 V) and 1.25 V versus a standard calomel electrode (SCE) with 30 min per step and data collection at 0.5-s intervals. Spectroscopic characterization was performed with a StellarNet EPP2000 concave grating UV-vis-NIR spectrophotometer with a tungsten krypton light source.

For controlled release experiments, films were formed by using radiolabeled ^{14}C-DS (100 μCi, 1.5 μCi/mg) dipping solution at a concentration of ≈4 μCi/ml. The LbL deposition procedure was then performed as described above. After deposition, ^{14}C-DS-labeled films were immersed in 40 ml of 10 mM KCl, and electrochemical deconstruction was performed by applying square wave potentials, also as described above. In all cases, films were first immersed for 10 min before application of potential, and minimal passive release was observed. A 1-ml sample was extracted at indicated time points and analyzed for radioactive ^{14}C content by adding 5 ml of ScintiSafe Plus 50% (Fisher Scientific) before measurement. Raw data (disintegrations per min per ml, DPM/ml) were converted to μg/ml ^{14}C-DS by using the conversion factor 2.2×10^6 DPM = 1 μCi = 0.67 mg of ^{14}C-DS. Finally, the total DS release from a single film was calculated according to the following equation:

$$M_i = C_i \times V_i + (1\ \text{ml}) \sum_{j=1}^{i-1} C_j, \qquad [1]$$

where M_i (μg) is the total cumulative mass released from the film as of measurement i, C_i (μg/ml) is the concentration of sample i, V_i (ml) is the total volume of the deconstruction bath before measurement i, and (1 ml)$\sum_{j=1}^{i-1} C_j$ is the total mass in previously extracted samples.

Cell viability assays were performed in triplicate by using the following protocol. All materials, buffers, and reagents were sterilized before use. Cell culture reagents were purchased from Invitrogen, and MTT viability assay kits were obtained from American Type Culture Collection. Focus HCC cells were grown in 96-well plates at an initial seeding density of 5,000 cells per well in 150 μl per well growth medium (90% modified Eagle's medium supplemented with 10% FBS, 100 units/ml penicillin, and 100 μg/ml streptomycin, 0.1 mM nonessential amino acids, 1 mM sodium pyruvate, and 2 mM L-glutamine). HeLa cells were grown in 96-well plates at an initial seeding density of 10,000 cells per well in 150 μl per well growth medium (90% modified Eagle's medium supplemented with 10% FBS, 100 units/ml penicillin, and 100 μg/ml streptomycin, 0.1 mM nonessential amino acids, 1 mM sodium pyruvate, and 2 mM L-glutamine). Cos-7 cells were grown in 96-well plates at an initial seeding density of 15,000 cells per well in 150 μl per well growth medium (90% Dulbecco's modified Eagle's medium supplemented with 10% FBS, 100 units/ml penicillin, and 100 μg/ml streptomycin). After seeding, cells were allowed to attach and proliferate for 24 h in an incubator (37°C, 5% CO_2). A sterile, 10× concentrated PBS buffer solution was added to an aqueous suspension of PB nanoparticles to yield a final solution containing 1.125 mg/ml PB, 137 mM NaCl, 2.7 mM KCl, and 10 mM Na_2HPO_4 at pH 7.4. Growth media were removed from cells and replaced with the above suspension of PB particles diluted in Opti-MEM (Invitrogen) at concentrations ranging from 0 mg/ml to 1.0 mg/ml PB. In parallel, cells were also incubated with carrier solutions alone (Opti-MEM plus an equivalent concentration of PBS without PB particles) to account for toxicity associated with the carrier solution only. Cells were incubated with the solutions for 4 h, after which solutions were removed and replaced with growth media. After 72 h, cell metabolic activity was assayed by using the MTT cell proliferation assay kit (American Type Culture Collection). Initially, a 10-μl aliquot of MTT assay reagent was added to each well. After incubating for 2 h, 100 μl of detergent reagent was added. The plate was then covered and left in the dark for 4 h, after which optical absorbance was measured at 570 nm by using a SpectraMax 190 microplate reader (Molecular Devices). Background (media plus MTT assay reagent plus detergent reagent with no cells present) was subtracted from the value of each well, and all values were normalized to the value of control (untreated) cells. In a similar fashion, the toxicity of an equivalent amount of PBS buffer in Opti-MEM (with no PB) was calculated. Values reported in Fig. 5 represent the normalized viability of PB-treated cells divided by the normalized viability of cells treated with equivalent amounts of pure PBS (to account for the toxicity of PBS itself).

ACKNOWLEDGMENTS. Special appreciation is extended to Dr. Dean DeLongchamp for helpful advice and discussions, and to Prof. Robert Langer (Massachusetts Institute of Technology) for the use of the scintillation counter in his laboratory. K.C.W. thanks the National Cancer Institute and the Massachusetts Institute of Technology Center for Cancer Research for a Ludwig Fellowship in Cancer Research. B.J.A. thanks the CMSE/MPC Summer Undergraduate Research Program at the Massachusetts Institute of Technology for an undergraduate research fellowship. This work was supported by the Bayer Professorship in Chemical Engineering at the Massachusetts Institute of Technology, the Division of Materials Research of the National Science Foundation (Grant DMR 99-03380), the Office of Naval Research, and the Institute for Soldier Nanotechnologies at the Massachusetts Institute of Technology under U.S. Army Research Office Contract DAAD-19-02D-0002.

1. LaVan DA, McGuire T, Langer R (2003) *Nat Biotechnol* 21:1184–1191.
2. Santini JT, Richards AC, Scheidt R, Cima MJ, Langer R (2000) *Angew Chem Int Ed* 39:2396–2407.
3. Santini JT, Cima MJ, Langer R (1999) *Nature* 397:335–338.
4. Razzacki SZ, Thwar PK, Yang M, Ugaz VM, Burns MA (2004) *Adv Drug Deliv Rev* 56:185–198.
5. Staples M, Daniel K, Cima MJ, Langer R (2006) *Pharm Res* 23:847–863.
6. Reed ML, Wu C, Kneller J, Watkins S, Vorp DA, Nadeem A, Weiss LE, Rebello K, Mescher M, Smith AJC, *et al.* (1998) *J Pharm Sci* 87:1387–1394.
7. Duffy DC, McDonald JC, Schueller OJA, Whitesides GM (1998) *Anal Chem* 70:4947–4984.
8. Decher G (1997) *Science* 277:1232–1237.
9. Hammond PT (2000) *Colloid Interface Sci* 4:430–432.
10. Hammond PT (2004) *Adv Mater* 16:1271–1293.
11. Tang Z, Wang Y, Podsiadlo P, Kotov NA (2006) *Adv Mater* 18:3203–3224.
12. Caruso F, Schuler C (2000) *Langmuir* 16:9595–9603.
13. Shi X, Caruso F (2001) *Langmuir* 17:2036–2042.
14. Sukhorukov GB, Brumen M, Donath E, Möhwald H (1999) *J Phys Chem B* 103:6434–6440.
15. Sukhorukov GB, Möhwald H (2004) in *Colloids and Colloid Assemblies*, ed Caruso F (Wiley, Weinheim, Germany), p 259.
16. Jewell CM, Zhang J, Fredin NJ, Lynn DM (2005) *J Controlled Release* 106:214–223.
17. Vazquez E, DeWitt DM, Hammond PT, Lynn DM (2002) *J Am Chem Soc* 124:13992–13993.

18. Wood KC, Boedicker JQ, Lynn DM, Hammond PT (2005) *Langmuir* 21:1603–1609.
19. Zhang J, Chua LS, Lynn DM (2004) *Langmuir* 20:8015–8021.
20. Chung AJ, Rubner MF (2002) *Langmuir* 18:1176–1183.
21. Hiller JA, Rubner MF (2003) *Macromolecules* 36:4078–4083.
22. Ma Y, Dong WF, Hempenius MA, Möhwald H, Vancso GJ (2006) *Nat Mater* 5:724–729.
23. Schuler C, Caruso F (2001) *Biomacromolecules* 2:921–926.
24. Wood KC, Chuang HF, Batten RD, Lynn DM, Hammond PT (2006) *Proc Natl Acad Sci USA* 103:10207–10212.
25. Boulmedais F, Tang CS, Keller B, Voros J (2006) *Adv Funct Mater* 16:63–70.
26. Mortimer RJ (1993) *Chem Soc Rev* 26:147–156.
27. Karyakin AA, Gltelmacher OV, Karyakin EE (1995) *Anal Chem* 67:2419–2423.
28. Mingotaud C, Lafuente C, Amiell J, Delhaes P (1999) *Langmuir* 15:289–292.
29. Neff VD (1978) *J Electrochem Soc* 125:886–887.
30. DeLongchamp DM, Hammond PT (2004) *Adv Funct Mater* 14:224–232.
31. Sukhishvili S, Granick S (2000) *J Am Chem Soc* 122:9550–9551.
32. Hansen MB, Nielsen SE, Berg K (1989) *J Immunol Methods* 119:203–210.
33. Wood KC, Little SR, Langer R, Hammond PT (2005) *Angew Chem Int Ed* 44:6704–6708.
34. Pearce J (1994) *Food Chem Toxicol* 32:577–582.